Cancer Letters 469 (2020) 78–88

Contents lists available at ScienceDirect

Cancer Letters

journal homepage: www.elsevier.com/locate/canlet

Original Articles

Three-dimensional oxabicycloheptene sulfonate targets the homologous recombination and repair programmes through estrogen receptor α antagonism

Jun Wu[a,1], Jing Yan[b,1], Pingping Fang[b], Hai-bing Zhou[c], Kaiwei Liang[b,d,e,**], Jian Huang[a,*]

[a] Hubei Key Laboratory of Cell Homeostasis, College of Life Sciences, Wuhan University, Wuhan, Hubei, 430072, China
[b] Department of Pathophysiology, School of Basic Medical Sciences, Wuhan University, Wuhan, 430071, China
[c] School of Pharmaceutical Sciences, Wuhan University, Wuhan, Hubei, 430071, China
[d] Research Center for Medicine and Structural Biology, School of Basic Medical Sciences, Wuhan University, Wuhan, 430071, China
[e] Hubei Province Key Laboratory of Allergy and Immunology, School of Basic Medical Sciences, Wuhan University, Wuhan, 430071, China

ARTICLE INFO

Keywords:
Selective estrogen receptor modulators (SERM)
Poly (ADP-ribose) polymerase (PARP)
Olaparib
RNA polymerase II (Pol II)
Synthetic lethality

ABSTRACT

Selective estrogen receptor modulators (SERMs) are a class of structurally diverse compounds, which have been extensively used to treat hormone-responsive cancers due to their unique partially agonistic and antagonistic properties toward estrogen receptors. Our previous studies have identified a three-dimensional SERM, oxabicycloheptene sulfonate (OBHS), as an estrogen receptor α (ERα) ligand, which is effective for the prevention and treatment of estrogen-dependent endometriosis *in vivo*. Here, using genome-wide ChIP-seq and RNA-seq analysis, we report that OBHS rapidly induces genome-wide ERα occupancy and acts as a partial agonist and antagonist for ERα. Interestingly, OBHS downregulates the homologous recombination and repair (HRR) modules, resulting in increased DNA damage, apoptosis and cell cycle arrest, inducing synthetic lethality with poly (ADP-ribose) polymerase (PARP) inhibitor olaparib through ERα antagonism. Mechanistically, OBHS impairs the RNA polymerase II (Pol II) loading at the promoters of estrogen-responsive HRR genes. Furthermore, combination therapy of OBHS with olaparib significantly reduces the tumour burden and delays the progression of breast cancer *in vivo*. Together, our studies not only characterise a novel SERM which uniquely targets the homologous recombination and repair programmes through ERα antagonism but also propose a synthetic lethal strategy by combining OBHS with PARP inhibitor olaparib for ERα-responsive cancers.

1. Introduction

Selective estrogen receptor modulators (SERMs) are a class of compounds which interact with estrogen receptor α or β (ERα or ERβ) and behave differently from the pure agonist 17β-estradiol through their unique ability to inhibit or stimulate estrogen-like action in various tissues [1,2]. SERMs have been widely used in multiple estrogen-related diseases, including infertility, postmenopausal osteoporosis, endometriosis, Alzheimer's disease and breast cancer. Breast cancer is the most common malignancy among women, and approximately 70% of breast cancer patients are characterised as ERα-positive. The proliferation of ERα-positive breast cancer cells depends on the signals from estrogen, thereby rendering them sensitive to ERα antagonists, such as tamoxifen [3]. However, long-term administration of tamoxifen results in drug resistance [4,5] and increased risk of endometrial carcinoma caused by tamoxifen's agonistic effects on endometrial cells [6]. Therefore, there is an urgent demand for developing new SERMs for breast cancer and other estrogen-related cancers.

Genetic analysis of breast cancer has identified the mutation of homologous recombination and repair genes, such as the well-known

Abbreviations: OBHS, Oxabicycloheptene sulfonate; SERM, Selective Estrogen Receptor Modulators; PARP, Poly (ADP-ribose) polymerase; HRR, Homologous recombination and repair; ERα, Estrogen receptor α; ERβ, Estrogen receptor β; DDR, DNA damage repair; ChIP-seq, Chromatin immunoprecipitations sequencing; RNA-seq, RNA sequencing; Pol II, RNA Polymerase II; NTD, N-terminal domain; SSB, Single-strand breaks; DAPI, 4′,6-diamidino-2-phenylindole; CI, Combination index

* Corresponding author.
** Corresponding author. School of Basic Medical Sciences, Wuhan University, Wuhan, Hubei, 430071, PR China.
E-mail addresses: kwliang@whu.edu.cn (K. Liang), jianhuang@whu.edu.cn (J. Huang).
[1] Equal contribution.

https://doi.org/10.1016/j.canlet.2019.10.019
Received 28 February 2019; Received in revised form 10 October 2019; Accepted 11 October 2019

BRCA1 and *BRCA2* genes, as vulnerable factors for the development of estrogen-related breast cancer and ovarian cancer, suggesting that the defect in DNA damage repair (DDR) contributes to the malignancy of tumours [7–9]. There are multiple DDR pathways to respond and restore different DNA damages, such as direct reversal repair, mismatch repair, base excision repair, nucleotide excision repair, homologous recombination and non-homologous end-joining [10]. Interestingly, the functional loss of one DDR pathway may be compensated by another compensatory DDR pathway, which results in an associated DDR dependency and offers the potential for a greater therapeutic window by tailoring treatment according to the lacking specific DDR functions [11]. For example, BRCA-mutated breast cancer cells have deficient homologous recombination repair pathways termed “BRCAness” [12], which depend on poly (ADP-ribose) polymerase (PARP)-mediated base excision repair for survival. Thus, inhibition of PARP is a promising strategy to selectively target BRCAness cancer cells by inactivating complementary DNA repair pathways, representing a synthetic lethal strategy. The PARP inhibitor olaparib represents the first medicine for BRCA-mutated breast cancer and ovarian cancer based on the synthetic lethality between PARP and BRCA1/2 [13]. However, the somatic BRCA mutation rate in breast cancer is low, and the non-BRCA-mutated breast cancer is generally not sensitive to PARP inhibitors, which much limit its application as a general therapeutic agent in breast cancer treatment.

Previously, we identified a novel SERM compound, oxabicycloheptene sulfonate (OBHS) (exo-5,6-Bis-(4-hydroxyphenyl)-7-oxabicyclo[2.2.1]hept-5-ene-2-sulfonic acid phenyl ester), with bridged oxabicyclic cores containing a diarylethylene motif [14]. OBHS has a unique three-dimensional structure compared to the two-dimensional estrogen, and it functions as a partial agonist and antagonist for ERα [14]. During the interaction of SERM to ERα, the change of helix 12 position in ERα is the critical event to determine the interaction of ERα with coactivators or corepressors, thereby, resulting in the partial agonism or antagonism of SERMs. Interestingly, different from the direct communication between tamoxifen and helix 12, OBHS interacts with the helix 11 of ERα and thereby modulates helix 12 indirectly through the distortion of helix 11 [15]. Due to the particular conformation of OBHS-ERα complex, OBHS has been reported to exert ERα antagonism in endometrial cells in contrast to the agonistic effects by tamoxifen and has shown anti-inflammatory effects in the occurrence and progression of endometriosis *in vivo* [16], suggesting that OBHS is a promising SERM for ERα antagonism in clinical application.

Here, with chromatin immunoprecipitations sequencing (ChIP-seq) and RNA sequencing (RNA-seq) analysis, we report that OBHS acts as a partial agonist and antagonist for ERα on the whole genome scale and induces a unique gene expression profile which is distinct from the full agonist 17β-estradiol. We found that OBHS induces BRCAness by downregulation of the homologous recombination and repair (HRR) modules, rendering its synergistic effects with PARP inhibitors and genotoxic doxorubicin. Furthermore, the combination of OBHS and PARP inhibitors reduces the tumour burden of breast cancer *in vivo*. Together, our studies have demonstrated that OBHS induces BRCAness through ERα antagonism and impairment of HRR modules and proposed a synthetic lethal strategy by combining OBHS with PARP inhibitors for ERα-responsive cancers.

2. Materials and methods

2.1. Chemicals and reagents

The compound OBHS was designed and synthesised as described previously [14]. 17β-estradiol was purchased from Sigma-Aldrich. PARP inhibitor olaparib and topoisomerase II inhibitor doxorubicin were obtained from Selleck Chemicals. Dimethyl sulfoxide (DMSO, Sigma-Aldrich) was used to dissolve all the chemicals. Mouse monoclonal anti-β-Actin antibody was purchased from Sigma-Aldrich. Purified anti-H2A.X Phospho (Ser139) antibody (clone 2F3) was obtained from BioLegend. Pol II RPB1 NTD antibody (D8L4Y), BCL-2 (50E3, #2870), BAX (#2772), Estrogen Receptor α (D8H8, #8644), and MCL-1 (D5V5L, #39224) were purchased from Cell Signaling Technology. ERα depletion was performed with three independent pSuper.retro.puro shRNAs. The targeting sequences are: 5′-ACAGGAG GAAGAGCTGCCA-3’ (shERα-1), 5′-TTGTGTTTCAACATTCTCC-3’ (shERα-2) and 5′-ATGCTGTACAGATGCTCCA-3’ (shERα-3). The scrambled shRNA (shScr) 5′-GCACTACTGTCGATGACGA-3′ was used as a negative control.

2.2. Cell culture

MCF-7, SK-OV-3, MDA-MB-231, HEK293T, T47D and Vero cells were purchased from the China Center for Type Culture Collection and were confirmed with short tandem repeat DNA profiling. These cell lines were maintained in Dulbecco's modified Eagle's medium supplemented with 10% fetal bovine serum and 1% penicillin/streptomycin. At least three days before use, cells were switched to phenol red-free Dulbecco's modified Eagle's medium containing 10% charcoal-stripped fetal bovine serum (Biowest by Rue de la Caille, France) and 1% penicillin/streptomycin. All cells were cultured at 37 °C in a 5% CO_2 humidified incubator.

2.3. Colony formation assay

Cells were seeded in 6-well culture plates with a density of 100 cells per well and treated with compounds at the indicated doses for two weeks. The medium was changed every two or three days with fresh compounds. Subsequently, the plates were gently washed with the phosphate-buffered solution (PBS) and were stained with the 3-(4,5-dimethylthiazol-2-yl)-2,5-diphenyl tetrazolium bromide at a final concentration of 1 mg/mL for 4 h. The stained colonies were dissolved with DMSO, and the absorption of 570 nm was measured using a BioTek microplate reader. Combination index (CI) of each combined drug group (such as drug A and drug B) was calculated using this formula: $CI = (E_A + (1\text{-}E_A)*E_B)/E_{A+B}$, where ‘E’ stands for the drug efficacy and $E = 1\text{-}OD_{drug}/OD_{vehicle}$. A CI of less than, equal to, and more than 1 (Log_2CI less than, equal to, and more than 0) indicates synergy, additivity and antagonism, respectively [17].

2.4. Flow cytometric analysis

For cell cycle analysis, MCF-7 cells were harvested and fixed gently with 75% pre-cooled ethanol overnight at 4 °C. The fixed cells were then washed with ice-cold PBS and then stained with propidium iodide in the presence of RNase A. The cells were measured by FACSCalibur flow cytometer, and the data were analysed by FlowJo 7.6. To measure the apoptosis in MCF-7 after compound treatments, MCF-7 cells were stained with the BD Annexin V-FITC apoptosis detection kit according to the manufacture's protocol. The apoptotic cells were measured by a FACSCalibur flow cytometer and analysed by the Beckman Summit 4.3 software.

2.5. Dual-luciferase reporter assay

Cells were seeded into a 48-well plate and were co-transfected with 300 ng of pGL3-TK-3ERE and 2 ng of pRL-CMV using EndoFectin™-Max transfection reagents according to the manufacturer's instruction. Twenty-four hours later, the cells were treated with compounds at the indicated concentrations for 24 h. The reporter gene activity was measured by the Promega Dual-Luciferase Reporter Assay System according to the manufacturer's protocol.

2.6. Chromatin immunoprecipitation sequencing (ChIP-seq)

Chromatin immunoprecipitation sequencing (ChIP-seq) was performed according to a previously published protocol [18]. Briefly, MCF-7 cells were fixed with 1% paraformaldehyde for 10 min and then quenched with glycine for 5 min at room temperature. Cross-linked chromatin was sonicated for 6 min and immunoprecipitated with the anti-ERα or Pol II NTD antibody and Dynabeads Protein G. Libraries were prepared with the HTP Library Preparation Kit for Illumina (KAPA Biosystems) and sequenced on a NextSeq 500. ChIP-seq reads were aligned to the human genome (UCSC hg19) with Bowtie version 1.1.2, allowing only uniquely mapping reads with up to two mismatches within the 50 bp read. The resulting reads were extended to 150 bp toward the interior of the sequenced fragment and normalised to total reads aligned (reads per million, r.p.m.). ERα and Pol II peaks were called using MACS (model-based analysis of ChIP-Seq) [19] version 1.4.2 using default parameters and were annotated with ChIPseeker. The ERα motif analysis was performed with MEME-ChIP. Heatmap and metagene plots were made for the indicated windows around the transcription start site (TSS) using the average coverage (r.p.m.).

2.7. Total RNA sequencing (RNA-seq)

After vehicle, OBHS and 17β-estradiol treatment for 12 h, MCF-7 cells were used for total RNA extraction. The extracted RNA was applied for DNase I digestion to remove the genomic DNA before RNA clean-up. The ribosomal RNA was depleted with Ribo-Zero rRNA removal kit and used for RNA-seq library preparation. The RNA-seq reads were aligned to human genome hg19 with TopHat with the default setting. The read counts across each gene were counted with HT-seq, and Deseq2 were used to analyse the differentially expressed genes. The heatmap was generated by R package 3.4.3 with normalised counts from Deseq2. Gene ontology (GO) analysis was performed using the Metascape online tool (http://metascape.org) [20].

2.8. Real-time quantitative PCR (RT-qPCR)

Total RNA was extracted as described above, and 1 μg of total RNA was used for reverse transcription with M-MLV reverse transcriptase and random hexamer primers. The synthesised cDNA was used for qPCR reaction performed on a CFX Connect™ Real-Time System with the SuperReal PreMix Plus (SYBR Green). The amplification primers for target genes were described as follows: *β-actin*: 5′-GATCATTGCTCCTC CTGAGC -3’ (Forward) and 5′-GTCATAGTCCGCCTAGAAGCAT-3’ (Reverse); *BRCA1*: 5′-CTCGCTGAGACTTCCTGGAC-3’ (Forward) and 5′-TCAACTCCAGACAGATGGGAC-3’ (Reverse); *BRCA2*: 5′-TCGTGCTT TGCAAGATGGTG-3’ (Forward) and 5′-TGTTCAGCAGATTCCATGGC-3’ (Reverse).

2.9. Laser scanning confocal microscopy

MCF-7 cells were fixed in 3.7% formaldehyde for 20 min at room temperature. After washing four times with ice-cold PBS, cells were permeabilized with PBS with 1% BSA and 0.1% v/v Triton-100 for 10 min at room temperature. Then cells were incubated with the primary antibodies diluted in PBS with 1% BSA and 0.1% v/v Triton-100 at 4 °C. After washing four times with PBS, cells were further incubated with Dylight 488 goat anti-mouse immunoglobulin G (lgG) and sealed on the glass slide using sealer containing 1 μg/mL of 4′,6-diamidino-2-phenylindole (DAPI, Sigma-Aldrich). Cell images were captured with a Leica TCS SP8 confocal microscope.

2.10. MCF-7 xenograft mouse model

MCF-7 xenograft mouse model was established as previously reported. Briefly, four-week-old female athymic mice (nu/nu genotype, BALB/c background) were purchased from Charles River (Beijing, China) and housed under aseptic conditions. All operations described below were performed following the laboratory animal guidelines of Wuhan University and were approved by the Animal Experimentations Ethics Committee of Wuhan University. To establish the MCF-7 xenograft, 1×10^7, 5×10^6, 2.5×10^6 MCF-7 cells, in 0.1 mL of cell culture media with Matrigel (BD Bioscience) were injected in the mammary pad of mice under anaesthetisation by isoflurane. Next, 2 mg/kg estradiol valerate was administered intramuscularly every week to maintain the hormone levels and stimulate the MCF-7 tumour growth. Immunohistochemistry and H&E staining were performed to confirm the tumour. For the *in vivo* therapy-response study, mice were randomly assigned to the vehicle (DMSO), OBHS, olaparib and OBHS-olaparib combination groups (n = 6 for each group) when the size of the tumour reached 100 mm^3. Mice were treated with drug administration by intraperitoneal injection at 25 mg/kg of olaparib and 100 mg/kg of OBHS, with once-daily administration for seven consecutive days. The tumour sizes were measured every day during treatment with calliper measurement. The tumour volume was calculated using the formula volume = (length × width × width)/2, and the mice were euthanised when the tumour size reached 1000 mm^3.

2.11. Statistical analysis

Data were represented as mean ± S.D. or mean ± S.E.M as stated. Statistical analysis was performed using one-way analysis of variance (ANOVA) followed by Bonferroni's ad post-hoc tests or two-way ANOVA with Tukey's test as indicated in the figure legends using Prism 7.0 software. Differences were considered statistically significant at $p < 0.05$ (*), $p < 0.01$ (**) and $p < 0.001$ (***).

3. Results

3.1. OBHS is a selective estrogen receptor modulator inducing genome-wide occupancy of ERα

Previously, we identified an ERα ligand, OBHS (7-oxabicyclo[2.2.1] hept-5-ene sulfonate), possessing a unique three-dimensional structure based on a bridged oxabicyclic core (Fig. 1A) [14]. OBHS indirectly modulates the helix 12 of ERα to induce a conformational change allowing the agonism and antagonism properties of ERα [15]. Importantly, compared to tamoxifen-mediated ERα agonism in endometrial cells, OBHS has been demonstrated to be effective in the treatment of endometriosis *in vivo* through ERα antagonism [16]. To better characterise OBHS, we first confirmed that OBHS could induce the ERα-ERE (estrogen-responsive element) [21] reporter gene expression in both MCF-7 and SK-OV-3 cells with ectopic expression of ERα (Fig. 1B–C, Figs. S1A and S1B), which is consistent with the previous studies that reported that OBHS acts as a partial agonist in a simple ERE reporter gene system [14]. Furthermore, we treated ERα-positive MCF-7 cells with OBHS and 17β-estradiol shortly for 1 h and performed the ERα ChIP-seq. We have found that stimulation of MCF-7 cells with OBHS or 17β-estradiol rapidly induces the chromatin recruitment of ERα as shown in the well-known estrogen-responsive genes, such as *GREB1*, *TFF1, IGFBP4* and *TKSU* (Fig. 1D and Fig. S1C) [22]. Genome-wide analysis of ERα peaks identified 1355, 15006 and 12612 peaks in the vehicle-, 17β-estradiol- and OBHS-treated conditions, respectively (Fig. 1E).

Annotation of these OBHS-induced peaks shows that the majority of them are intronic and distal intronic, which is consistent with the enhancer propriety of ERα binding sites (Fig. 1F and Fig. S1D). OBHS is generally weaker than 17β-estradiol in the induction of ERα binding genome-widely (Fig. 1G). The majority of OBHS-induced ERα peaks are overlapped with 17β-estradiol-stimulated ERα peaks, suggesting that OBHS is potentially competitive with 17β-estradiol in the induction of ERα binding to chromatin (Fig. 1H–I). We also noticed that OBHS and

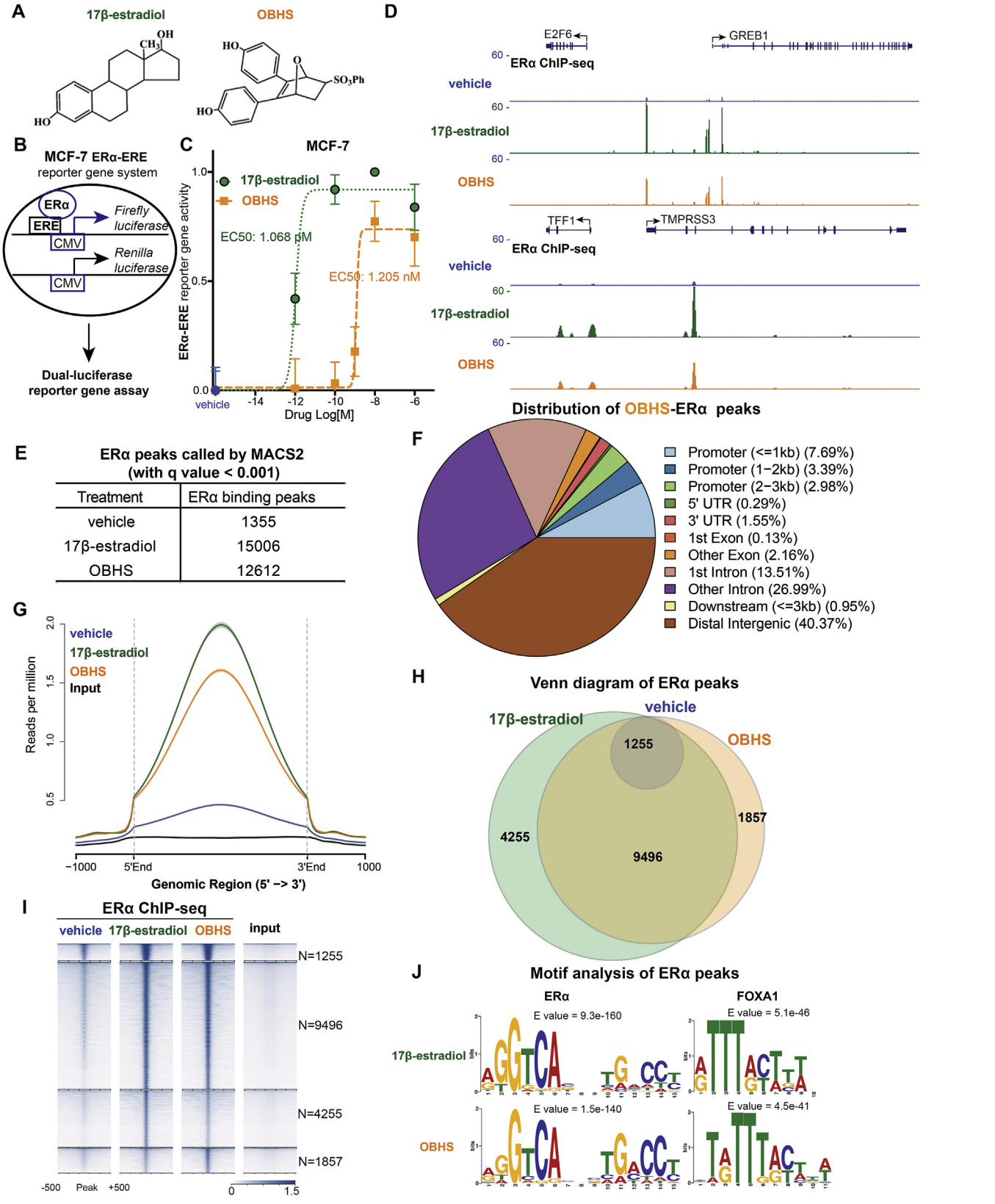

(caption on next page)

17β-estradiol prefer a small subset of peaks for ERα binding (Fig. 1H–I). Thus, we performed motif analysis of ERα peaks with MEME-ChIP. Consistent with previous reports [23], we have found that the ERα peaks are highly enriched in the motifs of ERα (ERE) and Forkhead Box A1 (FOXA1), which is a critical determinant of estrogen receptor function and endocrine response (Fig. 1J). Additionally, compared to 17β-estradiol-ERα, we have noticed that OBHS-ERα prefers a full ERE than a half ERE, and prefers to have a thymine nucleotide before

Fig. 1. Selective estrogen receptor modulator OBHS induces genome-wide occupancy of ERα. (A) Chemical structure of 17β-estradiol and three-dimensional selective estrogen receptor modulator OBHS. OBHS is a partial agonist and antagonist for ERα. (B) Illustration of ERα-ERE reporter gene assay in MCF-7 cells. pGL3-TK-3ERE and pRL-CMV plasmids were co-transfected into MCF-7 cells and then treated with different ER ligands. The firefly luciferase activity was measured with Promega Dual-Luciferase Reporter Gene Assay, while renilla luciferase activity served as a normalisation control. (C) ERα partial agonist OBHS dose-dependently activates ERα-ERE-mediated reporter gene expression. OBHS and 17β-estradiol induce ERα-ERE reporter gene expression with an EC50 of 1.205 nM and 1.068 pM, individually. (D) UCSC genome browser tracks of ERα ChIP-seq coverage in MCF-7 after OBHS and 17β-estradiol treatment. MCF-7 cells were treated with vehicle, 10 nM 17β-estradiol or 10 μM OBHS for 1 h before ERα ChIP-seq. The coverage (y-axis) was calculated as reads per million (r.p.m). (E-F) ERα peaks in MCF-7 cells after OBHS and 17β-estradiol treatment. ERα peaks were called by MACS2 and the number of peaks in each group was shown (E). Annotation of ERα peaks induced by OBHS, showing that most of the ERα peaks are intronic and distal intergenic (F). (G) OBHS is weaker than 17β-estradiol in the stimulation of genome-wide ERα occupancy in MCF-7 cells. ERα peaks from all three groups were merged, and the coverage of ERα was calculated with an extension of 1000 bp around the peak regions. (H) Proportional Venn diagram of ERα peaks in the vehicle-, OBHS- and 17β-estradiol-treated MCF-7 cells. (I) Heatmap of ERα occupancy at the ERα peaks in MCF-7 cells after vehicle, OBHS and 17β-estradiol treatment. Based on the overlapping of ERα peaks in the Venn diagram, the heatmap was divided into four different groups. (J) Motif analysis of ERα binding sites in OBHS- and 17β-estradiol-treated MCF-7 cells. ERα peak summits were extended to 50 bases and were used for MEME-ChIP to identify the ERα binding motifs. All three groups could identify the ERα and FOXA1 consensus motifs.

FOXA1 motif (Fig. 1J), which may explain the difference of ERα binding profiles between OBHS and 17β-estradiol.

3.2. Transcriptome analysis reveals that OBHS regulates a different gene expression profile than 17β-estradiol

We further tested OBHS in a panel of cells including the ERα-positive human breast cancer MCF-7 cells, ERβ-positive human ovarian SK-OV-3 cells, human triple-negative breast cancer MDA-MB-231 cells and control cell lines, African green monkey kidney Vero cells and human embryonic kidney HEK293T cells. We found that OBHS specifically inhibits the cell proliferation and colony formation in ERα-positive MCF-7 cells (Fig. S2A and Fig. 2A), which is consistent with the ERα preference and antagonism of OBHS [14] and suggests that OBHS is an antitumour compound for ERα-positive cancer cells. To obtain the gene expression profiles of OBHS in ERα-positive MCF-7 cells, we performed RNA-seq analysis with MCF-7 cells after OBHS or 17β-estradiol treatment for 12 h and identified the differentially expressed genes with Deseq2 (Fig. 2B–C). Analysis of these differentially expressed genes reveals that OBHS induces a different gene expression profile from 17β-estradiol (Fig. 2D and Fig. S2B). Interestingly, OBHS exhibits opposite effects of 17β-estradiol at the majority of target gene clusters as highlighted in Fig. 2D, suggesting that OBHS function as an ERα antagonist compared to the pure agonism of 17β-estradiol.

Gene ontology analysis [20] of the OBHS downregulated genes demonstrates that the cell cycle, chromosome segregation and maintenance, DNA replication and DNA damage repair related pathways are significantly enriched (Fig. 2E–F), while the upregulated genes by OBHS are enriched in cell stress responses, including response to endoplasmic reticulum stress, external stimulus, regulation of proteolysis, and stress-mediated transcriptional regulation (Figs. S2C and S2D). Furthermore, OBHS could arrest the cell cycle of MCF-7 cells at S phase (Fig. 2G–H) and induce the apoptosis in MCF-7 (Figs. S3A–D) along with the decreased protein expression of anti-apoptotic proteins BCL-2 and MCL-1 (Figs. S3E and S3F). These data are consistent with the RNA-seq analysis of OBHS, as well as the inhibitory effects of OBHS in cell proliferation and colony formation (Fig. S2A and Fig. 2A).

3.3. OBHS downregulates the homologous recombination repair and fanconi anemia pathway modules

Since the DNA damage repair pathways, such as the Fanconi anemia related genes [24], are downregulated in the gene ontology analysis, and OBHS induces cell stress and DNA replicating S phase arrest (Fig. 2), we used protein-protein interaction analysis [20] to further investigate the deregulated genes and found that OBHS significantly downregulates the homologous recombination repair (HRR) and Fanconi anemia pathway modules (Fig. 3A–B). These modules contain the well-known DNA damage repair genes *BRCA1* and *BRCA2,* as well as other HRR related genes. We performed RT-qPCR analysis and confirmed that OBHS decreases the mRNA expression levels of *BRCA1* and *BRCA2* genes in MCF-7 cells (Fig. 3C).

To study whether OBHS treatment results in the deficiency of DNA repair, we used Ser139 phosphorylated H2A.X (γH2A.X), which is a recognised fast-responding signal to double-strand breaks [25,26], and confocal microscopy to detect the deficiency of DNA repair after OBHS treatment. OBHS induces HRR deficiency as revealed by the γH2A.X Ser139 staining and confocal microscopy images (Fig. 3D). Analysis of the bulk level of γH2A.X Ser139 with increasing doses of OBHS confirmed that OBHS increases the γH2A.X Ser139 levels dose-dependently (Fig. 3E). Together, these data demonstrate that OBHS reduces HRR related genes expression and increases DNA damage in MCF-7 cells.

3.4. OBHS exerts synthetic lethality with PARP inhibitor olaparib through ERα antagonism

Given the paradigm of synthetic lethality between BRCA1/2 deficiency and PARP inhibition [13], we asked if OBHS could induce synthetic lethality in ERα-positive cancer cells, and whether this effect is mediated through ERα. Firstly, we confirmed the knockdown of ERα in MCF-7 cells by shRNAs, as shown in the Western blot analysis (Fig. S4A). Next, we studied the combined effects of OBHS with PARP inhibitor olaparib in MCF-7 cells after mock (shScr) or ERα knockdown (shERα). Because topoisomerase II inhibitor doxorubicin could generate the DNA double strand breaks, which requires BRCA1/2 for repair, we also tested the combined effects of OBHS with doxorubicin. As shown in Fig. 4A–B, OBHS exhibits synthetic lethality with olaparib (Fig. 4C–D) and doxorubicin (Fig. 4E–F) in the mock group (shScr), and the synthetic lethality is mediated through ERα since ERα knockdown itself sensitises the MCF-7 cells to olaparib and doxorubicin, and OBHS barely exerts additional inhibitory effects after ERα depletion (shERα). Interestingly, we also found that OBHS could decrease the mRNA level of ERα (Fig. S4B), suggesting that OBHS induces positive feedback to suppress ERα function. We also confirmed the downregulation of *ERα*, *BRCA1* and *BRCA2* in another ERα-positive breast cancer cell line T47D (Fig. S4C).

To measure the effects of OBHS with olaparib or doxorubicin, we calculated the combination index (CI) to distinguish the additive effect ($Log_2CI = 0$ or $CI = 1$) and synergism ($Log_2CI < 0$ or $CI < 1$). As shown in Fig. 4G, OBHS synergised with various concentrations of olaparib in inhibition of colony formation with the Log_2CI less than 0. After ERα knockdown, the drug-drug interaction of OBHS and olaparib switched to addictive effect confirming that ERα mediates the synergism of OBHS and olaparib. We also obtained similar synergistic effects of OBHS and olaparib in ERα-positive T47D cells (Fig. S4D). We also observed a similar but even stronger synergy between OBHS and doxorubicin, which is mediated by ERα blockage as well (Fig. 4H). Furthermore, we tested the effects of OBHS with olaparib (Figs. S4E and S4F) or doxorubicin (Figs. S4G and S4H) in ERα-negative Vero cells and found that there is no synergism in the ERα-negative Vero cells. Together, these results suggest that OBHS could inhibit ERα to synergise with PARP inhibitors or DNA topoisomerase II inhibitors.

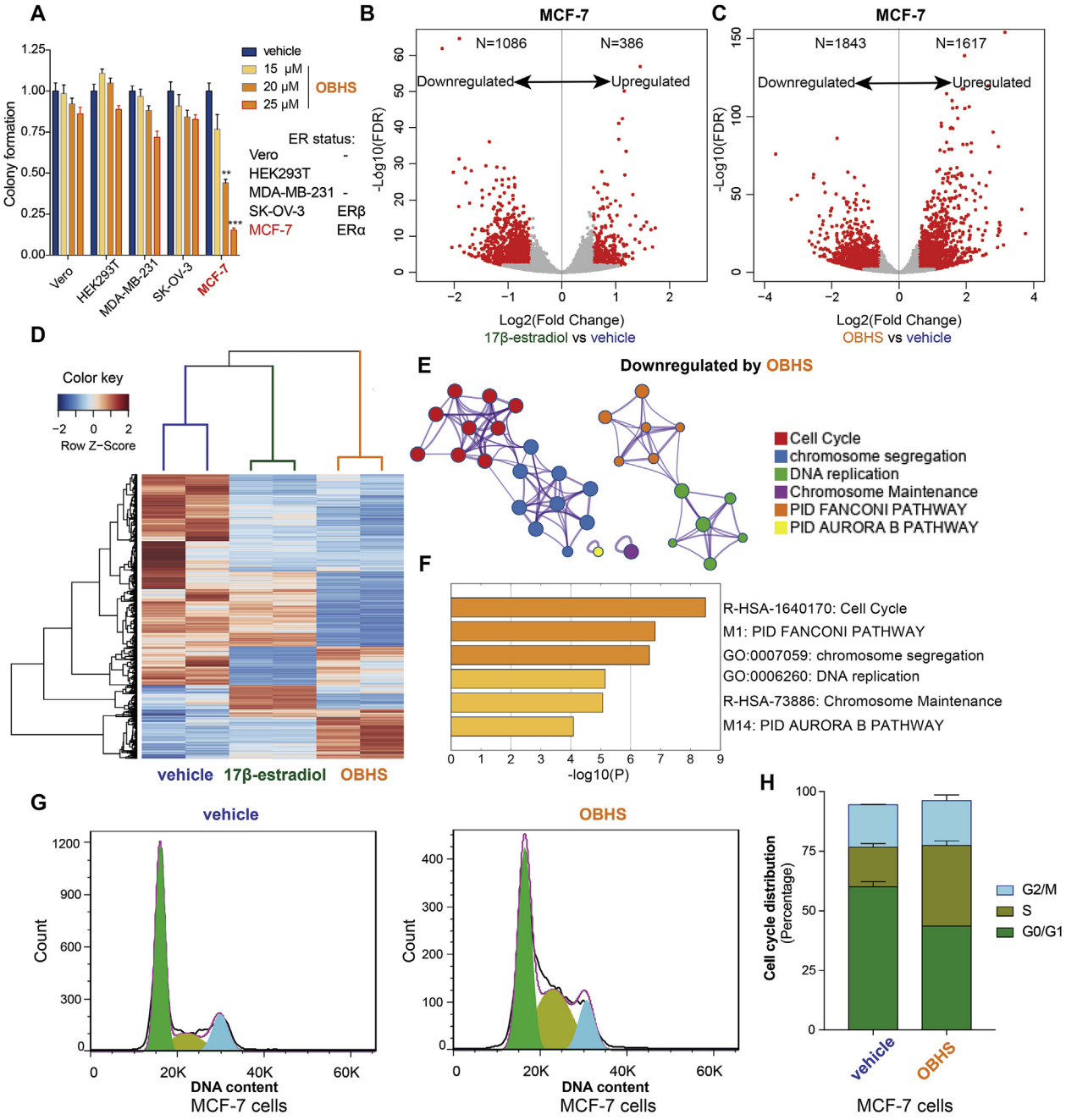

Fig. 2. Transcriptome analysis reveals that OBHS regulates a different gene expression profile than 17β-estradiol. (A) OBHS inhibits the colony formation of ERα positive MCF-7 cells. Vero (ERβ-, ERα-), HEK293T (ERβ-, ERα-), MDA-MB-231 (ERβ-, ERα-), SK-OV-3 (ERβ+, ERα-), and MCF-7 (ERβ-, ERα+) cells were treated with vehicle (DMSO), or increasing doses of OBHS, and the colonies were measured with MTT staining. Data were represented as mean ± S.D. One-way ANOVA analysis was used to calculate the significance with $^{**}p < 0.01$, $^{***}p < 0.001$. (B-C) Volcano plots of differentially expressed genes after 17β-estradiol or OBHS treatment for 12 h. The differentially expressed genes (fold change > 1.5, FDR < 0.01, and Log2CPM > 3) were highlighted with red dots. (D) Heatmap of differentially expressed genes showing that OBHS regulates a different gene expression profile from 17β-estradiol. (E-F) Gene ontology analysis of OBHS-down-regulated genes shows that the cell cycle, Fanconi pathway, chromosome segregation and maintenance and DNA replication terms are enriched. (G-H) OBHS induces cell cycle arrest at S phase in MCF-7 cells. MCF-7 cells were treated with vehicle or 20 μM OBHS for 24 h, and cell cycle alternations were measured with PI staining (G). The histograms represent the percentage of each cell cycle stage after vehicle or OBHS treatment (H). (For interpretation of the references to colour in this figure legend, the reader is referred to the Web version of this article.)

3.5. OBHS impairs the Pol II loading at the homologous recombination repair genes

The structural analysis of OBHS with ERα suggested that OBHS operates it antagonism by shifting ERα helix 11 and thereby indirectly altering the stability of ERα helix 12 into an antagonistic conformation [15]. To check the effects of OBHS-ERα in transcriptional regulation, we performed the RNA polymerase II (Pol II) ChIP-seq to investigate the mechanism for the inhibition of OBHS on HRR related genes. As shown in the UCSC genome browser tracks (Fig. 5A–C, Figs. S5A and S5B), ER agonist 17β-estradiol induces the increase of Pol II loading at these HRR genes, while OBHS reduces the Pol II loading at these genes, suggesting that the antagonist OBHS impairs the Pol II loading at the HRR genes. We also checked the genome-wide Pol II occupancy at all expressing

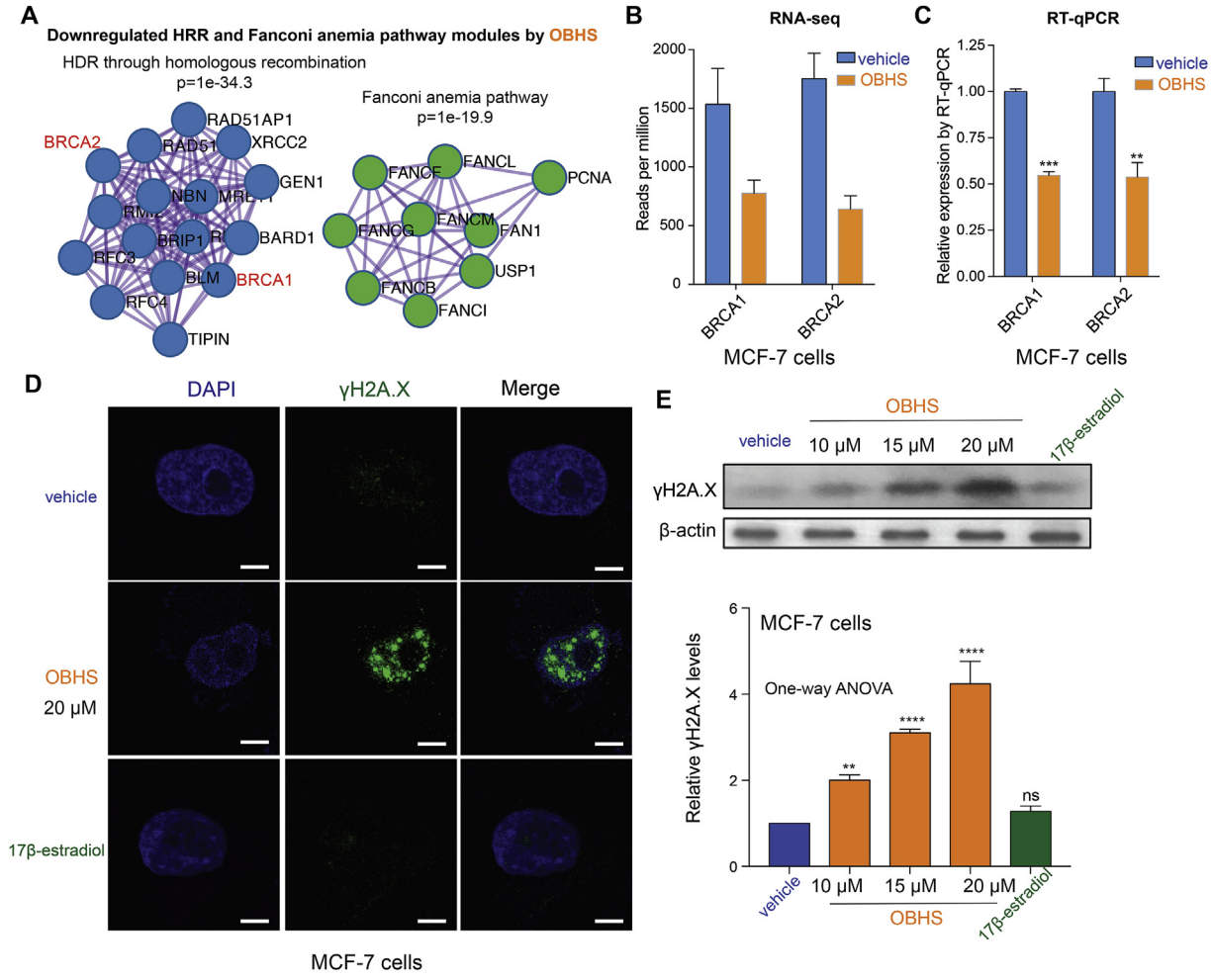

Fig. 3. OBHS downregulates the homologous recombination repair and Fanconi anemia pathway modules. (A) RNA-seq and protein-protein interaction analysis reveal that OBHS downregulates the homologous recombination repair and Fanconi anemia pathway modules. The example genes are highlighted in the cluster analysis, and these genes include the famous homologous recombination repair genes *BRCA1* and *BRCA2*. (B-C) *BRCA1* and *BRCA2* mRNA expression are decreased by OBHS, as revealed by both RNA-seq (B) and RT-qPCR (C). (D) OBHS induces homologous recombination repair deficiency as revealed by γH2A.X Ser139 staining and confocal microscopy images. MCF-7 cells were treated with vehicle, 20 μM OBHS or 10 nM 17β-estradiol for 4 h. The cells were then stained with anti-γH2A.X Ser139 antibody and followed by Dylight 488 conjugated secondary antibody and DAPI staining. The scale bar was 5 μm. (E) OBHS induces a bulk-level increase of γH2A.X Ser139 dose-dependently. MCF-7 cells were treated with vehicle, 10 nM 17β-estradiol and OBHS at indicated concentrations for 4 h before Western blot analysis. β-actin was used as a loading control. Quantification of γH2A.X Ser139 signals was shown in the bottom panel. Data were represented as mean ± S.D., and one-way ANOVA analysis was used to calculate the significance between vehicle- and compound-treated groups. ns: not significantly different, **p < 0.01, and ****p < 0.001.

genes and found that OBHS globally inhibits the Pol II occupancy around the TSS (Fig. S5C), suggesting that OBHS-ERα is compromised in loading Pol II to the promoters compared to 17β-estradiol-ERα. Furthermore, we analysed the reduced Pol II occupancy by OBHS genome-widely and identified 3075 genes with impaired Pol II loading, as shown in the heatmap (Fig. 5D).

Metaplot and boxplot analysis at the TSS of these 3075 genes showed that 17β-estradiol increases the Pol II loading, while OBHS impairs the Pol II loading at these genes (Fig. 5E–F), demonstrating that OBHS is an antagonist for ERα. We also noticed that the ERα agonist 17β-estradiol shows opposite effects of OBHS in Pol II loading at these 3075 genes (Fig. 5E), and 17β-estradiol increases the Pol II loading at the majority of the 3075 genes, of which the Pol II coverage is reduced by OBHS (Fig. S5D). Together, these results are consistent with the antagonism of OBHS and provide mechanistic insights of OBHS-mediated downregulation of HRR genes through impairment of Pol II loading at their promoter regions.

3.6. Combinational therapy of OBHS and olaparib delays breast cancer progression in vivo

To determine if OBHS and olaparib could be used *in vivo* as possible cancer therapeutics for ER, we established a murine MCF-7 tumour model (Figs. S6A and S6B) with the injection of MCF-7 cells into the mammary pad of four-week-old female athymic mice. Mice inoculated with increased amounts of MCF-7 cells developed larger tumours, which were further confirmed with Hematoxylin & Eosin staining and immunohistochemistry (Fig. S6C). In the following *in vivo* therapy-response study, we used 1×10^7 MCF-7 cells for the mammary pad injection to establish the MCF-7 breast xenograft tumour model.

To measure the potential of OBHS and olaparib in the MCF-7 tumour model, we initiated the injection of the animals with OBHS and olaparib on day 11 after inoculation, when the average tumour size reached 100 mm^3. The mice were administered once daily with OBHS and olaparib for seven days, and the tumour weights were monitored with caliper measurements (Fig. 6A and B). The mice were euthanised when the tumour size reached 1000 mm^3. One-week injection of OBHS

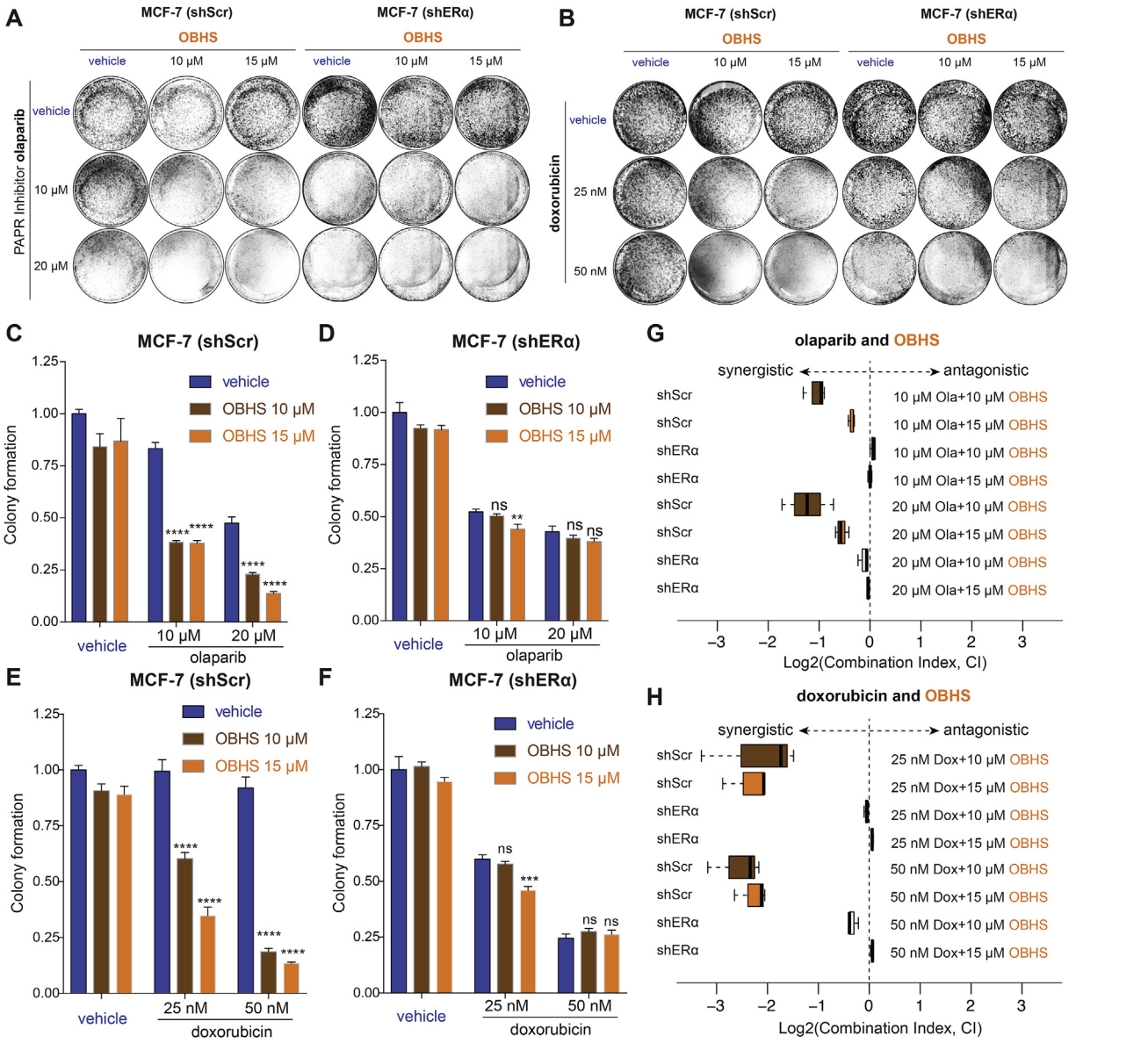

Fig. 4. OBHS exerts synthetic lethal effects with PARP inhibitor olaparib and genotoxic doxorubicin through ERα. (A-B) OBHS exerts synthetic lethal effects with olaparib and doxorubicin. After scramble or ERα shRNA knockdown, MCF-7 cells were seeded into 6-well plates and treated with OBHS in combination with PARP inhibitor olaparib (A) or genotoxic doxorubicin (B) at the indicated concentrations. One representative out of 3 biological replicates is shown. (C-D) ERα knockdown decreases the synthetic lethal effects of OBHS and olaparib. (E-F) ERα depletion impairs the synthetic lethal effects of OBHS and doxorubicin. (G-H) Combination index analysis of OBHS and olaparib (G), OBHS and doxorubicin (H) show that OBHS exhibits synergistic effects with olaparib and doxorubicin, and the synergistic effects are impaired after ERα depletion.

alone at the dosage of 100 mg/kg, which has no observed toxicity and does not result in significant effects on tumour growth compared to vehicle control (Fig. 6C and D). Olaparib has a minimal effect on tumour growth. However, the difference between olaparib and vehicle groups was not significant ($p = 0.102$). Interestingly, combination of olaparib and OBHS significantly delays tumour progression as monitored by tumour sizes ($p = 0.001$) (Fig. 6C and D). Together, these data suggest that combinational therapy of OBHS and olaparib delays breast cancer progression *in vivo*.

4. Discussion

In this study, we firstly reported the selective estrogen receptor module activity of a novel three-dimensional ligand, OBHS, which could rapidly induce genome-wide ERα occupancy (Fig. 1) and regulate a different gene expression profile compared to the full agonist 17β-estradiol (Fig. 2). Mechanistically, we revealed that OBHS impairs the Pol II loading at homologous recombination repair genes (Fig. 5) resulting in decreased expression of the homologous recombination repair pathway (Fig. 3). Furthermore, OBHS exerts synthetic lethal effects with olaparib and doxorubicin and delays the tumour progression *in vivo* (Figs. 4 and 6). OBHS produces two complementary results that together enhance the sensitivity to olaparib and doxorubicin: (1) OBHS reduces the well-known homologous recombination repair pathways, such as BRCA1 and BRCA2, which confer synthetic lethality with PARP inhibitors and genotoxic drugs; (2) OBHS decreases the expression of ERα, and knockdown of ERα sensitises breast cancer cells to olaparib and doxorubicin (Fig. 4).

PARP is crucially involved in the repair of single-strand breaks (SSBs), which can be blocked by PARP inhibitors. Unrepaired SSBs during DNA replication can be converted to more deleterious DNA double-strand breaks, which requires BRCA1/2 for DNA damage repair

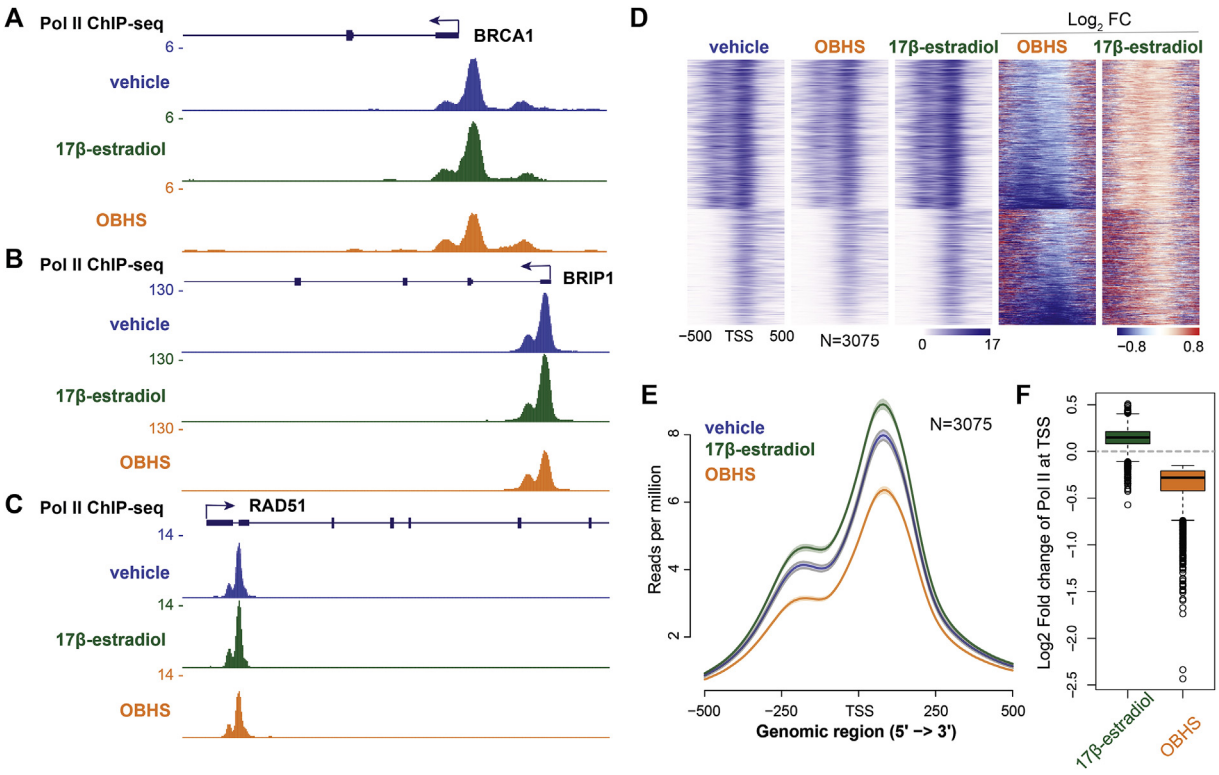

Fig. 5. OBHS impairs the Pol II loading at the homologous recombination repair genes. (A-C) UCSC genome browser tracks of Pol II ChIP-seq at homologous recombination repair genes after ligand treatments for 1 h. The Pol II coverage around the TSS of *BRCA1*, *BRIP1*, and *RAD51* is shown as reads per million. The Pol II loading at those loci is decreased by OBHS in 1 h, suggesting that OBHS rapidly impairs the Pol II initiation at the homologous recombination repair genes. (D) Identification of 3075 protein-coding genes with impaired Pol II loading in MCF-7 cells by OBHS. Coverage around the 1 kb window of TSS was calculated and plotted as long as the log2 fold changes versus the vehicle control. (E-F) Metaplot and boxplot of Pol II at the TSS sites of the 3075 genes in Fig. 5D show that 17β-estradiol increases the Pol II loading, while OBHS impairs the Pol II loading at these genes.

[27]. PARP inhibitors initially were found to cause synthetic lethality in cancer cells with BRCA1 or BRCA2 deficiencies [13] and have been approved by the Federal Drug Administration for various cancers with either germline or somatic mutations in BRCA1 and BRCA2. Additionally, PARP inhibitors trap the PARP1 and PARP2 enzymes at damaged DNA, leading to the formation of trapped PARP–DNA complexes [28]. Advances in the understanding of PARP inhibitors show that homologous recombination deficiency resulting from alterations of components other than BRCA1 or BRCA2 in the pathway also lead to increased sensitivity of cancer cells to PARP inhibitors. For example, PARP inhibitors induce significant killing of ataxia telangiectasia mutated (ATM)-deficient and phosphatase and tensin homolog (PTEN)-mutant cancer cells [29–31].

Here, we found that OBHS increases the double-strand breaks as revealed by γH2A.X staining and decreases the mRNA expression of *BRCA1*, *BRCA2* and other HRR related genes through repression of Pol II loading at those genes, suggesting that OBHS induces homologous recombination deficiency, which explains the synergistic effects of OBHS with olaparib and doxorubicin and agrees with the observed cell cycle arrest at S phase and increased apoptosis by OBHS. Interestingly, recently, Liu's group showed that tamoxifen-resistant breast cancer cells are resistant to DNA-damaging chemotherapy because of upregulated BRCA1 and BARD1, and inhibition of BARD1 and BRCA1 resensitize breast cancer cells to DNA-damaging chemotherapy both *in vitro* and *in vivo* [32]. Because OBHS could directly impair the expression of *BRCA1* and *BARD1* (Fig. 3A), we anticipate that OBHS has the potential to resensitise tamoxifen-resistant breast cancer cells to chemotherapy.

We characterised OBHS as a selective estrogen receptor module with partial agonistic and antagonistic properties of ERα. Although OBHS induces genome-wide ERα occupancy, which has almost the same binding motifs as 17β-estradiol-ERα, transcriptome analysis revealed that OBHS has different transcriptional profiles compared to 17β-estradiol. OBHS regulates a small subset of genes similar to 17β-estradiol; however, OBHS shows opposite effects on the majority of deregulated genes by 17β-estradiol (Fig. 2D). These data are consistent with the ERα partial agonistic and antagonistic properties, and also agree with the crystal structural analysis of OBHS-ERα, showing that OBHS utilises its antagonism by shifting ERα helix H11 in different directions and altering the stability of ERα helix 12 into the antagonistic conformer indirectly [15]. The structural insights also explain why OBHS and 17β-estradiol have opposite effects on Pol II loading at the homologous recombination repair genes. The synergistic effects of OBHS with olaparib and doxorubicin are likely to be caused by ERα antagonism because ERα-negative Vero cells show no synergistic effects of OBHS with olaparib and doxorubicin, and ERα knockdown in MCF-7 cells could sensitise MCF-7 cells to olaparib and doxorubicin. Together, inhibition of ERα by OBHS plays a crucial role in the synergistic effects of OBHS with olaparib and doxorubicin. Interestingly, we also found that OBHS could directly reduce the mRNA expression of ERα, which further enhances the synergy between OBHS and olaparib or doxorubicin.

In vivo application of OBHS in an endometriosis mouse model has shown that OBHS exerted suppression of estrogenic and inflammatory activities in the progression of endometriosis [16]. Here, we also showed that combination therapy of OBHS and olaparib significantly delays the tumour progression in ERα-positive breast cancer mouse model, which expanded the application of olaparib to breast cancer. Additionally, the three-dimensional structure of OBHS makes it elastic and variable in structure, thus, it could be further modified with other functional groups. For example, OBHS was chemically bonded with the pan-histone deacetylase inhibitor SAHA with some modifications, and a series of more potent antitumour dual-target conjugates were

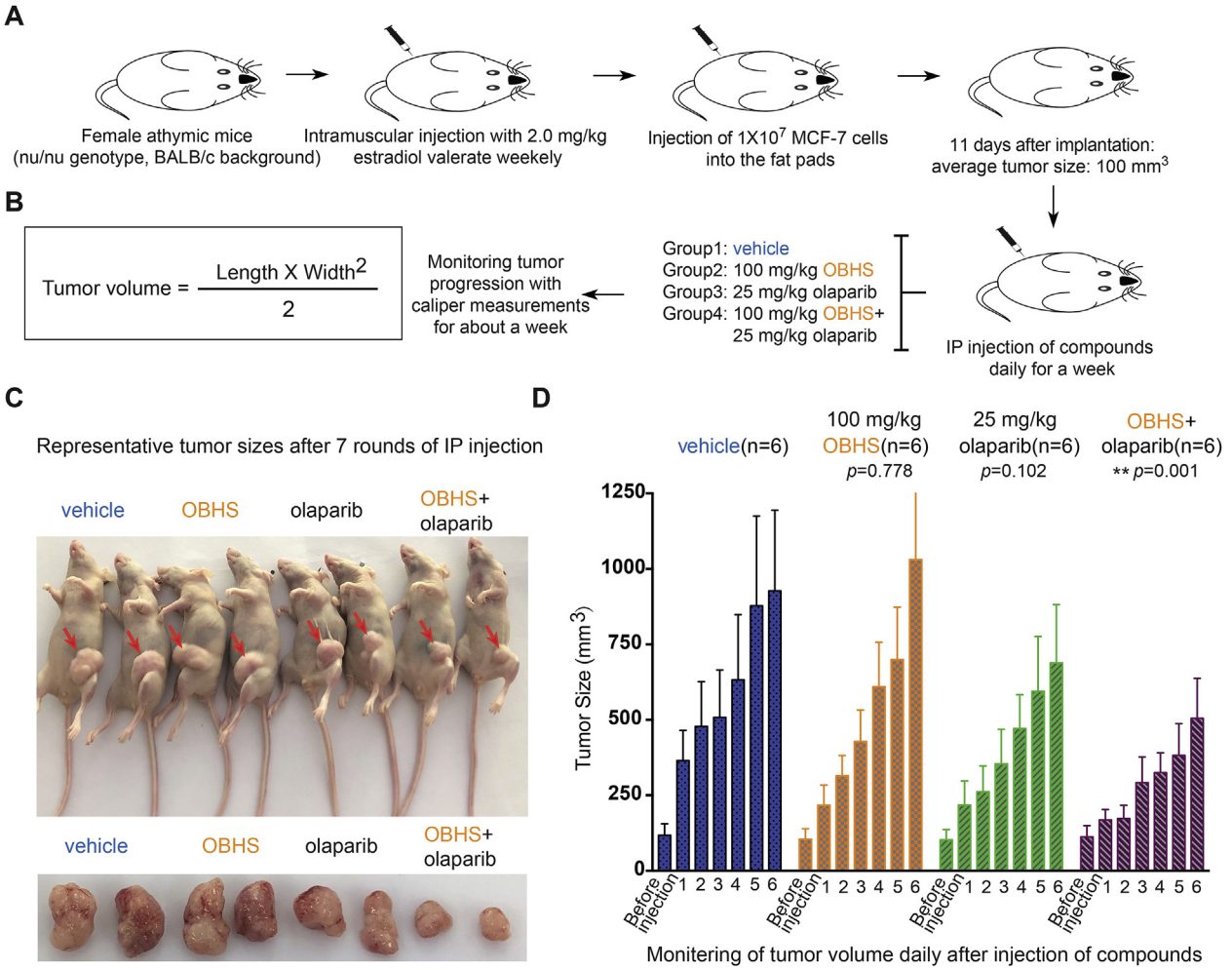

Fig. 6. Combination therapy of OBHS and PARP inhibitor olaparib significantly delays disease progression in the MCF-7 breast cancer mouse model. (A-B) Schematic of the development of MCF-7 tumours in athymic nude mice. Athymic nude mice were injected with 2 mg/kg estradiol valerate intramuscularly every week to maintain the hormone levels and stimulate the MCF-7 tumour growth. 1×10^7 MCF-7 cells were inoculated into the fat pads of nude mice. Eleven days after injection, when the average size of the tumour reached 100 mm^3, mice were divided randomly into four groups. Drug treatments were performed with once daily with vehicle, 100 mg/kg of OBHS, 25 mg/kg of olaparib or combination of OBHS (100 mg/kg) and olaparib (25 mg/kg) for a total of 7 intraperitoneal injections in a week (A). The tumour sizes were measured every day during treatment with calliper measurement and were calculated using the formula volume = (length × width × width)/2 (B). (C) Representative tumour sizes after seven rounds of drug treatment. (D) Combination of OBHS and olaparib delays the tumour growth in the MCF-7 tumour mouse model. The average tumour sizes of the vehicle- (n = 6), OBHS- (n = 6), olaparib- (n = 6) and combination therapy (n = 6)-treated groups were plotted from day 11 to day 18 after inoculation. Data were represented as Mean ± S.E.M, and the statistical analysis between vehicle- and drug-treated groups were performed by a two-way ANOVA analysis with Tukey's test. *p* values were indicated.

synthesised and tested in cancers [33,34]. Given the profound effects of OBHS with olaparib in ERα-positive breast cancer and the chemical property of OBHS, we are optimistic that OBHS and its derivatives could be potential antitumour candidates for breast cancers in combination with other DNA damaging agents through an alternative synthetic lethal strategy.

Authorship agreement

All co-authors agree to the submission to Cancer Letters and agree with the content and presentation of the paper.

Funding

This work was supported by the National Key Research and Development Program of China Stem Cell and Translational Research (NO. 2019YFA0111100 to Kaiwei Liang), National Natural Science Foundation of China (31870786, 31371331, 81573279, 81373255) and the National Basic Research Program of China (973 Program) (2012CB720600).

CRediT authorship contribution statement

Jun Wu: Methodology, Validation, Formal analysis, Investigation, Writing - original draft. **Jing Yan:** Methodology, Resources, Investigation, Validation. **Pingping Fang:** Methodology, Formal analysis, Writing - review & editing. **Hai-bing Zhou:** Methodology, Resources. **Kaiwei Liang:** Conceptualization, Validation, Formal analysis, Writing - review & editing, Supervision, Project administration, Funding acquisition, Visualization. **Jian Huang:** Writing - review & editing, Supervision, Conceptualization, Project administration, Funding acquisition.

Declaration of competing interest

The authors declare no conflict of interest.

Acknowledgments

We thank the core facility of the College of Life Sciences at Wuhan University for the flow cytometry and confocal microscopy assistance. The accession number for the raw and processed NGS data reported in this paper is GEO: GSE133941.

Appendix A. Supplementary data

Supplementary data to this article can be found online at https://doi.org/10.1016/j.canlet.2019.10.019.

References

[1] B.L. Riggs, L.C. Hartmann, Selective estrogen-receptor modulators – mechanisms of action and application to clinical practice, N. Engl. J. Med. 348 (2003) 618–629.
[2] C.K. Osborne, H. Zhao, S.A. Fuqua, Selective estrogen receptor modulators: structure, function, and clinical use, J. Clin. Oncol. 18 (2000) 3172–3186.
[3] S.W. Fanning, R. Jeselsohn, V. Dharmarajan, C.G. Mayne, M. Karimi, G. Buchwalter, et al., The SERM/SERD bazedoxifene disrupts ESR1 helix 12 to overcome acquired hormone resistance in breast cancer cells, Elife 7 (2018).
[4] W. Toy, Y. Shen, H. Won, B. Green, R.A. Sakr, M. Will, et al., ESR1 ligand-binding domain mutations in hormone-resistant breast cancer, Nat. Genet. 45 (2013) 1439–1445.
[5] S.W. Fanning, C.G. Mayne, V. Dharmarajan, K.E. Carlson, T.A. Martin, S.J. Novick, et al., Estrogen receptor alpha somatic mutations Y537S and D538G confer breast cancer endocrine resistance by stabilizing the activating function-2 binding conformation, Elife 5 (2016).
[6] Y. Shang, M. Brown, Molecular determinants for the tissue specificity of SERMs, Science 295 (2002) 2465–2468.
[7] Y. Miki, J. Swensen, D. Shattuck-Eidens, P.A. Futreal, K. Harshman, S. Tavtigian, et al., A strong candidate for the breast and ovarian cancer susceptibility gene BRCA1, Science 266 (1994) 66–71.
[8] L.H. Castilla, F.J. Couch, M.R. Erdos, K.F. Hoskins, K. Calzone, J.E. Garber, et al., Mutations in the BRCA1 gene in families with early-onset breast and ovarian cancer, Nat. Genet. 8 (1994) 387–391.
[9] A. Antoniou, P.D. Pharoah, S. Narod, H.A. Risch, J.E. Eyfjord, J.L. Hopper, et al., Average risks of breast and ovarian cancer associated with BRCA1 or BRCA2 mutations detected in case Series unselected for family history: a combined analysis of 22 studies, Am. J. Hum. Genet. 72 (2003) 1117–1130.
[10] S.P. Jackson, J. Bartek, The DNA-damage response in human biology and disease, Nature 461 (2009) 1071–1078.
[11] M.J. O'Connor, Targeting the DNA damage response in cancer, Mol. Cell 60 (2015) 547–560.
[12] C.J. Lord, A. Ashworth, BRCAness revisited, Nat. Rev. Cancer 16 (2016) 110–120.
[13] H. Farmer, N. McCabe, C.J. Lord, A.N. Tutt, D.A. Johnson, T.B. Richardson, et al., Targeting the DNA repair defect in BRCA mutant cells as a therapeutic strategy, Nature 434 (2005) 917–921.
[14] H.B. Zhou, J.S. Comninos, F. Stossi, B.S. Katzenellenbogen, J.A. Katzenellenbogen, Synthesis and evaluation of estrogen receptor ligands with bridged oxabicyclic cores containing a diarylethylene motif: estrogen antagonists of unusual structure, J. Med. Chem. 48 (2005) 7261–7274.
[15] N. Sharma, K.E. Carlson, J.C. Nwachukwu, S. Srinivasan, A. Sharma, K.W. Nettles, et al., Exploring the structural compliancy versus specificity of the estrogen receptor using isomeric three-dimensional ligands, ACS Chem. Biol. 12 (2017) 494–503.
[16] Y. Zhao, P. Gong, Y. Chen, J.C. Nwachukwu, S. Srinivasan, C. Ko, et al., Dual suppression of estrogenic and inflammatory activities for targeting of endometriosis, Sci. Transl. Med. 7 (2015) 271ra279.
[17] T.C. Chou, Theoretical basis, experimental design, and computerized simulation of synergism and antagonism in drug combination studies, Pharmacol. Rev. 58 (2006) 621–681.
[18] K. Liang, A.R. Woodfin, B.D. Slaughter, J.R. Unruh, A.C. Box, R.A. Rickels, et al., Mitotic transcriptional activation: clearance of actively engaged Pol II via transcriptional elongation control in mitosis, Mol. Cell 60 (2015) 435–445.
[19] Y. Zhang, T. Liu, C.A. Meyer, J. Eeckhoute, D.S. Johnson, B.E. Bernstein, et al., Model-based analysis of ChIP-seq (MACS), Genome Biol. 9 (2008) R137.
[20] S. Tripathi, M.O. Pohl, Y. Zhou, A. Rodriguez-Frandsen, G. Wang, D.A. Stein, et al., Meta- and orthogonal integration of influenza "OMICs" data defines a role for UBR4 in virus budding, Cell Host Microbe 18 (2015) 723–735.
[21] K. Liang, L. Yang, Z. Xiao, J. Huang, A bipartite recombinant yeast system for the identification of subtype-selective estrogen receptor ligands, Mol. Biotechnol. 41 (2009) 53–62.
[22] W.J. Welboren, M.A. van Driel, E.M. Janssen-Megens, S.J. van Heeringen, F.C. Sweep, P.N. Span, et al., ChIP-Seq of ERalpha and RNA polymerase II defines genes differentially responding to ligands, EMBO J. 28 (2009) 1418–1428.
[23] A. Hurtado, K.A. Holmes, C.S. Ross-Innes, D. Schmidt, J.S. Carroll, FOXA1 is a key determinant of estrogen receptor function and endocrine response, Nat. Genet. 43 (2011) 27–33.
[24] R. Ceccaldi, P. Sarangi, A.D. D'Andrea, The Fanconi anaemia pathway: new players and new functions, Nat. Rev. Mol. Cell Biol. 17 (2016) 337–349.
[25] J.A. Downs, S. Allard, O. Jobin-Robitaille, A. Javaheri, A. Auger, N. Bouchard, et al., Binding of chromatin-modifying activities to phosphorylated histone H2A at DNA damage sites, Mol. Cell 16 (2004) 979–990.
[26] L.J. Mah, A. El-Osta, T.C. Karagiannis, gammaH2AX: a sensitive molecular marker of DNA damage and repair, Leukemia 24 (2010) 679–686.
[27] A. Kuzminov, Single-strand interruptions in replicating chromosomes cause double-strand breaks, Proc. Natl. Acad. Sci. U.S.A. 98 (2001) 8241–8246.
[28] J. Murai, S.Y. Huang, B.B. Das, A. Renaud, Y. Zhang, J.H. Doroshow, et al., Trapping of PARP1 and PARP2 by clinical PARP inhibitors, Cancer Res. 72 (2012) 5588–5599.
[29] M.S. Gilardini Montani, A. Prodosmo, V. Stagni, D. Merli, L. Monteonofrio, V. Gatti, et al., ATM-depletion in breast cancer cells confers sensitivity to PARP inhibition, J. Exp. Clin. Cancer Res. 32 (2013) 95.
[30] A.M. Mendes-Pereira, S.A. Martin, R. Brough, A. McCarthy, J.R. Taylor, J.S. Kim, et al., Synthetic lethal targeting of PTEN mutant cells with PARP inhibitors, EMBO Mol. Med. 1 (2009) 315–322.
[31] V.J. Weston, C.E. Oldreive, A. Skowronska, D.G. Oscier, G. Pratt, M.J. Dyer, et al., The PARP inhibitor olaparib induces significant killing of ATM-deficient lymphoid tumor cells in vitro and in vivo, Blood 116 (2010) 4578–4587.
[32] Y. Zhu, Y. Liu, C. Zhang, J. Chu, Y. Wu, Y. Li, et al., Tamoxifen-resistant breast cancer cells are resistant to DNA-damaging chemotherapy because of upregulated BARD1 and BRCA1, Nat. Commun. 9 (2018) 1595.
[33] C. Tang, C. Li, S. Zhang, Z. Hu, J. Wu, C. Dong, et al., Novel bioactive hybrid compound dual targeting estrogen receptor and histone deacetylase for the treatment of breast cancer, J. Med. Chem. 58 (2015) 4550–4572.
[34] J. Dong, N. Zheng, X. Wang, C. Tang, P. Yan, H.B. Zhou, et al., A novel HDAC6 inhibitor exerts an anti-cancer effect by triggering cell cycle arrest and apoptosis in gastric cancer, Eur. J. Pharmacol. 828 (2018) 67–79.